Journal of Materials Chemistry A

Highly stable and active palladium nanoparticles supported on porous carbons for practical catalytic applications

Journal:	*Journal of Materials Chemistry A*
Manuscript ID:	TA-ART-06-2014-003097.R1
Article Type:	Paper
Date Submitted by the Author:	26-Jul-2014

Complete List of Authors:	Veerakumar, Pitchaimani; Academia Sinica, Institute of Atomic and Molecular Sciences Madhu, Rajesh; National Taipei University of Technology, Electroanalysis and Bioelectrochemistry Lab, Department of Chemical Engineering and Biotechnology CHEN, SHEN-MING; National Taipei University of Technology , Department of Chemical Engineering and Biotechnology Vediyappan, Veeramani; National Taipei University of Technology, Department of chemical Engineering and Biotechnology Hung, Chin-Te; Academia Sinica, Institute of Atomic and Molecular Sciences Tang, Pi-Hsi; Chung Cheng Institute of Technology, National Defense University, Department of Chemical and Materials Engineering Wang, Chen-Bin; Chung Cheng Institute of Technology, National Defense University, Liu, Shang-Bin; National Taiwan Normal University, Department of Chemistry

Cite this: DOI: 10.1039/c0xx00000x

www.rsc.org/xxxxxx

ARTICLE TYPE

Highly stable and active palladium nanoparticles supported on porous carbons for practical catalytic applications†

Pitchaimani Veerakumar,[#a] Rajesh Madhu,[#b] Shen-Ming Chen,[*b] Vediyappan Veeramani,[b] Chin-Te Hung,[a] Pi-Hsi Tang,[ac] Chen-Bin Wang[c] and Shang-Bin Liu[*ad]

Received (in XXX, XXX) Xth XXXXXXXXX 20XX, Accepted Xth XXXXXXXXX 20XX
DOI: 10.1039/b000000x

Carbon porous materials (CPMs) containing highly dispersed palladium nanoparticles (PdNPs) with average size of *ca.* 5 nm are synthesized by using microwave (MW) irradiation procedure, during which the Pd^{2+} ions were effectively reduced to Pd^{0} form and highly dispersed on the carbon support. The Pd/CPM samples were characterized by a variety of analytical and spectroscopy techniques, *viz.* N_2 adsorptio/desorption isotherm measurements, thermogravimetric analysis (TGA), X-ray diffraction (XRD), scanning and filed-emisstion electron microscopy (SEM/FETEM), Fourier transform infrared spectroscopy (FT-IR), and Raman spectroscopy. The Pd/CPM composites were employed as heterogeneous catalysts for reduction of 4-nitrophenol (4-NP) to 4-aminophenol (4-AP) in aqueous media. The reaction was monitored by using UV-Visible spectroscopy, yielding a pseudo-first-order rate constant (k) of 6.87×10^{-2} s^{-1}. Moreover, the catalysts were exploited for C–C coupling reactions using the microwave (MW) method. In addition, a novel electrochemical sensor for detection of 4-NP was developed based on a Pd/CPM-modified galssy carbon electrode (GCE) using the cyclic voltammetry (CV) and differential pulse voltammetry (DPV) methods. The 4-NP sensor was found to exhibit excellent sensitivity, lower detection limit, reliability, and durability surpassing the reported modified electrodes, rendering practical industrial applications.

1. Introduction

Carbon porous materials (CPMs) have played an increasingly critical role in scientific and industrial applications due to their tunable textural properties such as pore size, pore volume, and surface area, rendering a wide range of applications in materials sciences and chemistry,[1,2] for examples, as excellent adsorbents for fuel storage or as support materials for catalysts, sensors etc.[3,4]

The preparation and catalytic activity of transition metal nanoparticles (MNPs) supported on CPMs can be found in several recent reports.[5,6] The high surface area and large pore volume possessed by the CPM supports are known to be favorable for mass transfer while prevailing the confinement effect to prevent uncontrollable growth of the MNPs, thus, beneficial for catalytic reactions.[7,8] Several carbon precursors, such as phenolic resin (P-F resin), polysaccharide (PS), furfuryl alcohol (FA), and polydopamine (PDA), have been exploited for fabricating carbon nanostructures.[9,10] Moreover, palladium nanoparticles (PdNPs) have attracted considerable R&D attention due to their versatile catalytic properties for a wide variety of reactions such as Suzuki cross-coupling, hydrogenation, oxidation as well as specified applications in electrocatalysis, such as electrodes for sensors and fuel cells, etc.[11,12]

[a]*Institute of Atomic and Molecular Sciences, Academia Sinica, Taipei 10617, Taiwan. E-mail: sbliu@sinica.edu.tw*
[b]*Department of Chemical Engineering and Biotechnology, National Taipei University of Technology, Taipei 10608, Taiwan. E-mail: smchen78@ms15.hinet.net*
[c]*Department of Chemical and Materials Engineering, Chung Cheng Institute of Technology, National Defense University, Taoyuan 33449, Taiwan*
[d]*Department of Chemistry, National Taiwan Normal University, Taipei 11677, Taiwan*

†Electronic Supplementary Information (ESI) available: Experimental details, assorted experimental results obtained from TGA, XRD, FE-TEM, and UV-Vis studies. See DOI: 10.1039/c3anxxxxxx

[#]*These authors contributed equally*

Herein, we report a novel one-pot synthesis procedure to fabricate PdNPs supported on mesoscopic CPMs (Pd/CPM) by means of a soft-templating approach[13] using phloglucinol and formaldehyde as primary carbon precursors and palladium(II) acetylacetonate ($Pd(acac)_2$) as the metal precursor. A more detailed description of the synthsis procedures can be found in the Electronic Supplementary Information **(ESI†; Fig. S1)**. As shown in **Scheme 1**, the Pd/CPM catalyst may be obtained by pyrolizing the phloroglucinol–formaldehyde resin with the organometallic Pd precursor (which also serves as sencondary carbon source).[10a]

Recently, we employed CPM-modified glassy carbon electrodes (GCEs) for sensitive electrochemical detections of harzardous molecules such as 4-nitrophenol (4-NP) and dopamine (DA).[14] Nitrophenol and its derivatives are an important byproduct from the production of pesticides, herbicides, and synthetic dyes.[15] 4-NP is known to damage the central nervous system, liver, kidney and blood of animals and humans. Thus, effective removal of 4-NP from contaminated waste water is one of the most important environmental issues. Nonetheless, owing to the high stability and solubility of 4-NP in water, the treatment of 4-NP by traditional methods are mostly ineffective. Moreover, the reduction of 4-NP is also a demanding task in the pharmaceutical industries (*e.g.* manufacture of analgesic, antipyretic drugs, *etc.*), photographic developer, corrosion inhibitor, anticorrosion lubricant, etc.[16] It will be shown later that the Pd/CPM composite not only represents an effective catalyst for 4-NP reduction but also for C–C coupling reactions, as illustrated in **Scheme 1**. It is noteworthy that the Pd/CPM catalyst system reported herein aslo offers several advantages in terms of straightforward scale-up synthesis procedures, environmental-friendliness, and low cost. It is envisaged that the broad application of this approach should contribute to the development of next generation advanced catalytic materials.

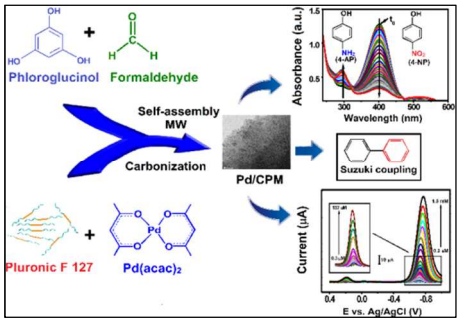

Scheme 1 Schematic illustrations of synthesis and applications of Pd/CPM catalyst system.

2. Results and discussion

2.1 Catalysts characterization

Fig. 1A displays the XRD patterns of pristine CPM, Pd/CPM-1 and, Pd/CPM-2 samples. The sharp diffraction peaks at $2\theta = 40.1^o$ (111), 46.5^o (200), 68.2^o (220), and 82.3^o (311) match well with the characteristic peaks of Pd (JCPDS, Card No. 05-0681),[17] whereas the broad peaks at $2\theta = 23.4^o$ (002) and 43.5^o (100) reveal the presence of graphitic carbons. An average particle size of ca. 5–8 nm was deduced for the PdNP by means of Scherrer equation based on the full-width half-maximum (FWHM) linewidth of the prominent (111) peak. The graphitic nature of the CPM support was further justified by the Raman spectra **(Fig. 1B)**, revealing a G and D bands at *ca.* 1590 and 1350 cm^{-1}, respectively, indicating the presences of in-plane vibration of sp^2 carbons as well as carbons with defect structures. The slightly stronger intensity observed for the D band than G band reflects amorphous nature of the graphized carbon network **(Table 1)**.[17a]

The N_2 adsorption/desorption isotherms obtained at 77 K for the pristine CPM and catalyst samples loaded with 0.5wt% (Pd/CPM-1) and 1.0 wt% (Pd/CPM-2) Pd^0 metal **(Figs. 1C)** exhibit the typical type IV isotherms (*cf.* IUPAC classification) with signiture hysteresis loops revealing the presence of mesoporosity in the carbon substrates, as also revealed by the BJH pore size distributions **(Fig. 1D)**.[8] The sharp adsorption curves at the Henry's Law region indicate the co-existence of microporosity in there samples. The textural properties of so determined for various samples are depicted in **Table 1.**

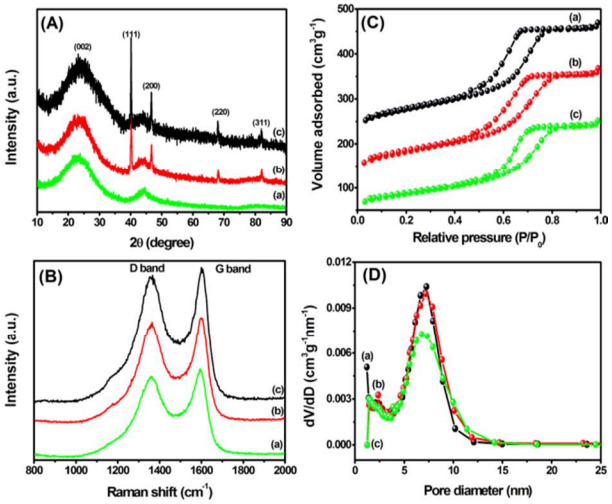

Fig. 1 (A) XRD patterns, (B) Raman spectra, (C) N_2 adsorption/desorption isotherms, and (D) BJH pore size distributions of (a) pristine CPM, (b) Pd/CPM-1, and (c) Pd/CPM-2 samples.

Table 1 Textural properties of the pristine CPM and Pd/CPM materials

Sample	Pd loading (wt%)	Pd size (nm)[a]	Surface area ($m^2\ g^{-1}$)[b]		Pore volume ($cm^3\ g^{-1}$)[c]			Pore size (nm)[f]	I_G/I_D
			S_{Total}	S_{Micro}[d]	V_{Total}	V_{Micro}[d]	V_{Meso}[e]		
CPM	---	---	744	411	0.53	0.31	0.22	5.1	0.99
Pd/CPM-1	0.1	5.1 ± 0.2	608	218	0.52	0.09	0.43	4.9	0.98
Pd/CPM-2	0.5	5.1 ± 0.5	432	178	0.48	0.07	0.41	5.9	0.89

[a] Average Pd particle size determined by FE-TEM analysis. [b] Brunauer–Emmet–Teller (BET) surface areas. [c] Total pore volumes calculated as the amount of N_2 adsorbed at P/P_0 is 0.99. [d] Microporous surface areas (S_{Micro}) and pore volumes (V_{Micro}) obtained from t-plot analyses. [e] Mesopore volume ($V_{meso} = V_{Total} - V_{micro}$. [f] Pore diameters calculated by the Barrett–Joyner–Halenda (BJH) method using adsorption branches of isotherms.

Compared to the parent CPM, the Pd/CPM-1 and Pd/CPM-2 composite materials show slightly lower surface areas and pore volumes, as anticipated due to the incorporation of PdNPs.[3,4,7,8] Further experiments by field-emission transmission electron microscopy (FE-TEM) reveal the wormhole-like mesoporous structure of CPMs and well-dispersed PdNPs within the mesopors of Pd/CPM-1 with an average diameter of 5.1 ± 0.2 nm **(Figs. 2b and 2c)**, as confirmed by the selected-area electron diffraction (SAED) pattern shown in **Fig. 2b (Inset)**, which shows distict (111), (200), (220), and (311) planes anticipated for the face-centered cubic (fcc) structure of Pd metal. Similar results may be inferred for the distribution of PdNPs in Pd/CPM-2 **(Fig. S2A; ESI†)**. That the observed particle sizes are comparable to the average pore size of the CPM indicating a homogeneously distribution of PdNPs within the mesopores of the carbon support.

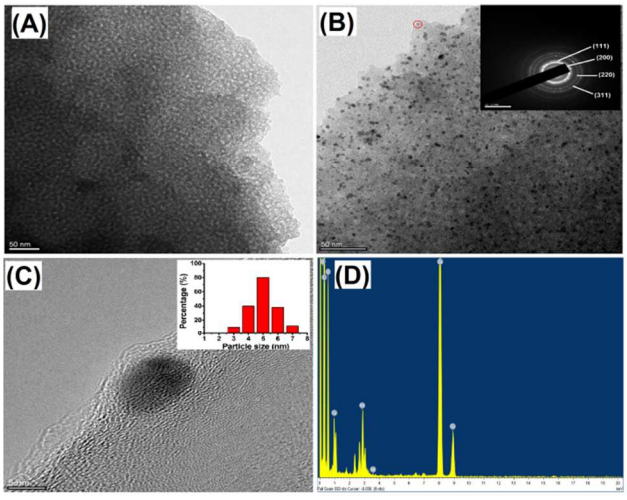

Fig. 2 FETEM images of (a) pristine CPM and (b)-(c) Pd/CPM-1 composite and (d) its corresponding EDX spectrum. Insets in (b) and (c) show the SAED pattern and histogram of PdNP of the Pd/CPM-1 catalyst.

The elemental composition of the powdered Pd/CPM composite samples was further examined by EDAX, which revealed an intensed signal in the Pd region **(Fig. 2d)**. Metallic PdNPs typically exhibits an optical absorption peak at *ca.* 2.80 keV due to surface plasmon resonance.[17b] On the basis of FE-TEM and SAED results, it is indicative that PdNPs are mostly in the form of sphereical single crystals with an average diameter of ca. 5 nm. The thermal stability of the Pd/CPM composits were further examined by thermogravimetric analysis (TGA). Similar to the pristine CPM, the Pd-loaded CPMs also exhibit two distinct weight-loss peaks at 50–150 and 400–650 °C, corresponding to a weight loss of 8% and 75–80%, respectively **(see Fig. S2C, ESI†)**. The peak appeared at lower temperature may be attributed to the desorption of physisorbed water and organic solvent, whereas the high-termperature peak should be associated with the weightloss of carbon support.[18]

2.2 Reduction of 4-NP over Pd/CPM catalysts

To assess the catalytic activity of Pd/CPM catalyst during reduction of 4-NP, test reactions were carried out by mixing aqueous solution of 4-NP (1×10^{-4} M) with an reducing agent, namely $NaBH_4$ (1.3 M). Upon adding peroper amount of Pd/CPM catalyst, the reaction was monitored by UV-Vis spectroscopy. Relavent experimental details may be found in **ESI† (Fig. S3)**. In brief, upon adding $NaBH_4$ into the aqueous 4-NP (ligh yellow color), the reaction suspension immediately undergoes a redshift from 318 to 400 nm, indicating the formation of 4-nitrophenolate ion (4-Nip; dark yellow), as shown in **Fig. 3a**.[19] On the other hand, after introducing *ca.* 2 mg of Pd/CPM-1 catalyst into the above reaction mixture, a consistent decrease in absorption peak intensity at 400 nm with time occurred, indicating a successive

reduction of 4-Nip **(Fig. 3b)**. This is accompanied by the appearance of a new absorption peak at 300 nm, whose intensity increases progressively with time, indicating the anticipated formation of 4-aminophenol (4-AP). On the other hand, even in the presence of strong reducing agent $NaBH_4$, the intensity and wavelength of the peak responsible for 4-Nip (at 400 nm) remained nearly unchanged when in the absence of a catalyst **(Fig. S4c, ESI†)**. Since porous carbon alone cannot catalyze the reduction of 4-NP, it is conclusive that the supported PdNPs catalyst are responsible for the observed catalytic activity. Similar phenomena were observed when in the presence of Pd/CPM-2 catalyst having a higher Pd loading (1.0 wt%).

To determine the reaction rate, we monitored variations of absorption peak intensity of 4-Nip with time in the presence of a Pd/CPM catalysts. Taking Pd/CPM-1 as an example, prior to the catalytic reduction of 4-Nip, an initinal induction period (t_o) of *ca.* 4.5 s was observed **(Fig. 3c)**. After the induction period, a consistent decrease in the absorption peak intensity with time was observed. In this context, since the concentration of $NaBH_4$ was much higher than that of 4-NP, the reduction kinetics is most suitable to be described by the pseudo first-order reaction with respect to 4-NP alone. **Fig. 3d** shows the variation of $\ln(A/A_o)$ versus reaction time for the reduction 4-NP, where A and A_o represents absorption peak intensity of 4-Nip at time t and 0, respectively. In agreement with results obtained from a previous

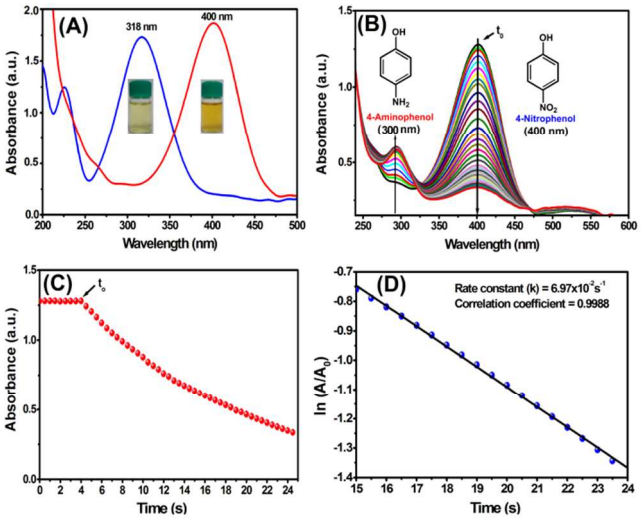

Fig. 3 (A) UV-Vis spectra obtained from aqueous 4-NP before (blue curve) and after (red curve) the addition of $NaBH_4$ solution. (B) Successive reduction of 4-Nip (aqueous 4-NP in $NaBH_4$) in the presence of Pd/CPM-1 catalyst. (C) Variations of absorption peak intensity for 4-Nip at 400 nm with time under an induction period t_o = 4.5 s. (D) linear relationship of $\ln(A/A_0)$ as a function of time. The slope of the plot $\ln(A_0/A)$ *vs* t (sec) gives the reaction rate constant ($k = 6.97 \times 10^{-2} s^{-1}$) was obtained directly from the slope.

study,[20] the kinetics of 4-NP reduction (in $NaBH_4$) may be expressed by the linear equation: $\ln(A_o/A) = kt$. Accordingly, the corresponding rate constant (k) associated with Pd/CPM-1 and Pd/CPM-2 during reduction of 4-NP may be deduced as 6.97×10^{-2} and 6.77×10^{-2} s^{-1}, respectively, which is superior compare to those reported in the literature (**Table 2**). For examples, comparing with the k values obtained from reduction of 4-NP over the Pd/graphene (6.6×10^{-3} s^{-1})[21f] and Pd/CNT ($0.2–2.0 \times 10^{-2}$ s^{-1})[21a] catalysts with similar Pd particle size (*ca.* 3–7 nm), the Pd/CPM catalysts reported herein show superior and comparable catalytic activities.

Based on a previously proposed scheme,[14b,22] the mechanism for reduction of 4-NP in presence of $NaBH_4$ over the Pd/CPM catalyst is illustrated in **Scheme 2**. Accordingly, the catalytic reduction of 4-NP over Pd/CPM is provoked by electron transfer from BH_4^- to 4-NP through adsorption of the reactant molecules onto the surfaces of the catalyst (Step I). The catalytic activity is known to depend on the surface area of the Pd/CPM catalysts as well as the mass transfer resistant of the reactant.[14b,22c] The latter if clearly benefit by the mesoscopic properties (*i.e.,* porous size, surface area, and pore volume) of the CPM support. The reduction of 4-NP, which is the rate-determining step, is provoked by interaction of adsorbed 4-NP with hydrogen atoms bound on active surfaces of PdNPs (Steps II and III). As a result of reduction reaction, 4-AP is form, followed by desorption of product from the metal surfaces (Step IV) and reactivation of the Pd/CPM catalytic system.[22d]

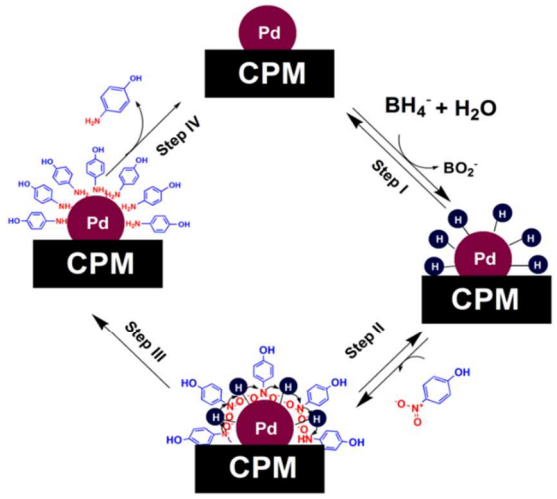

Scheme 2. The proposed mechanism of the reduction of the 4-NP by $NaBH_4$ using Pd/CPM catalyst.

Table 2 Comparison of apparent rate constants for 4-NP reduction over various Pd supported catalyst systems

Catalyst	PdNP particle size (nm)	Catalyst amount (mg)	Recation time (s)	Rate constant k (s^{-1})	Reference
Pd/G[a]	15–20	2.0 (mL)	720	2.35×10^{-3}	5a
Pd/CNT[b]	1.5 ± 0.4	50	420	1.05×10^{-2}	5c
Pd/CNT	2.7	0.05 (mL)	3,600	$0.17–2.0 \times 10^{-2}$	21a
Pd/C[c]	3.4	7.2 (mM)	720	8.83×10^{-3}	21b
Pd/oMWCNT[d]	2.3	1.0	210	---	21c
RGO[e]@Pd@C	4.0	5.0	30	---	21d
Pd/GO[f]	4.4	0.25	120	34.3×10^{-3}	21e
Pd/G	6.6	4.0	90	36.5×10^{-3}	21f
Pd/CPM-1	5.1 ± 0.2	2.0	25	6.97×10^{-2}	This work
Pd/CPM-2	5.1 ± 0.5	2.0	25	6.77×10^{-2}	This work

[a] G: graphene. [b] CNT: carbon nanotubes. [c] C: sponge-like amorphous carbon. [d] oMWCNT: oxidized multi-wall carbon nanotubes. [e] RGO: reduced graphene oxide. [f] GO: graphene oxide.

2.3 Suzuki-Miyaura coupling reaction over Pd/CPM catalysts

The Suzuki–Miyaura coupling reaction is one of the most useful methods for selective C–C bond formation for the construction of bi-aryl skeletons, which are often included as partial structures, especially in pharmaceuticals, natural products, industrial raw materials and functional materials.[23] The Pd/CPM catalysts were exploited for C–C bond formation *via* coupling of different aryl halides with phenylboronic acid under mild conditions **(Table S1, ESI†)**. The results clearly show that such heterogeneous catalysts also exhibit superior catalytic activities for C–C coupling reactions with desirable product yields > 88% in the presence of 5.0 mg Pd/CPM-2 catalyst (Pd loading 1.0 wt%). By comparison, inferior product yields (> 82%) was observe when Pd/CPM-1 is applied. For examples, over the Pd/CPM-2 catalyst, Suzuki reaction invoking iodobenzene (Ph-I) and phenylboronic acid ($PhB(OH)_2$), leading to a biphenyl (Ph-Ph) yield of 99% within 10 min at 100 °C under microwave (MW) irradiation. On the other hand, over the Pd/CPM-2 catalyst, conversions of bromobenzene (Ph-Br) and chlorobenzene (Ph-Cl) led to a biphenyl yield of 95% and 88%, respectively, wihin 15 min MW irradiation **(Table S1, ESI†)**. Whereas, a somewhat lower yields biphenyl were observed over the Pd/CPM-1 catalyst. Moreover, the effect of catalyst amount on screening of the C-C coupling reactions was also examined **(Table S2, ESI†)**. We have achieved 99% yield of biphenyl, when Ph-I reacts with phenylboronic acid under the mild reaction conditions: Pd/CPM-2 catalyst weight > 5 mg; aryl halide, 1.0 mmol; phenylboronic acid, 1.2 mmol; K_2CO_3, 2 mmol; aqueous dimethylformamide (DMF : H_2O = 1 : 1), 5 mL; temperature, 100 °C; duration, 10 min; MW power, 300 W. Most importantly, the catalyst can be easily recovered from the reaction mixture by centrifugation. The structure and morphology of the recycled spent catalysts remained practically intact, as verified by the FE-TEM and XRD results shown in **Figs. S2B and S2D (ESI†)**.

2.4 Electrochemical detection of 4-NP by Pd/CPM-modified GCE

To evaluate the electrocatalytic activity of the Pd/CPM-1 modified glassy carbon electrode (GCE), cyclic voltammograms (CVs) were recorded for the bare and Pd/CPM-1 modified GCEs with and without the presence of 4-NP in acetate buffer solution. As shown in **Fig. 4A**, no redox peak was observed at Pd/CPM-1 modified GCE in the absence of 4-NP **(Fig. 4A, curve b)**. Upon adding 0.3 mM 4-NP in 10 mL of 0.05 M acetate buffer solution (pH 5), featureless CV curve was observed for the bare GCE **(Fig. 4A, curve a)**, revealing a relatively weak current peak (I_{pc} = 3 μA) at cathodic peak potential E_{pc} = −0.8 V. In this case, the presence of the cathodic peak may be attributed to reduction of nitryl group of the 4-NP to form 4-hydroxylaminophenol through a $4e^-/4H^+$ transfer electrochemical reduction process.[24-26] On the other hand, a notable redox peak at 0.16 V with a strong reduction peak (E_{pc})

at –0.7 V and cathodic peak current I_{pc} = 29 μA was observed for the Pd/CPM-1 modified GCE. It is noteworthy that, compared to the bre GCE, the I_{pc} value obtained for the Pd/CPM-1 modified electrode increased by nearly 10 folds, while a much lower reduction overpotential of 4-NP with a positive shift of 100 mV was also observed.

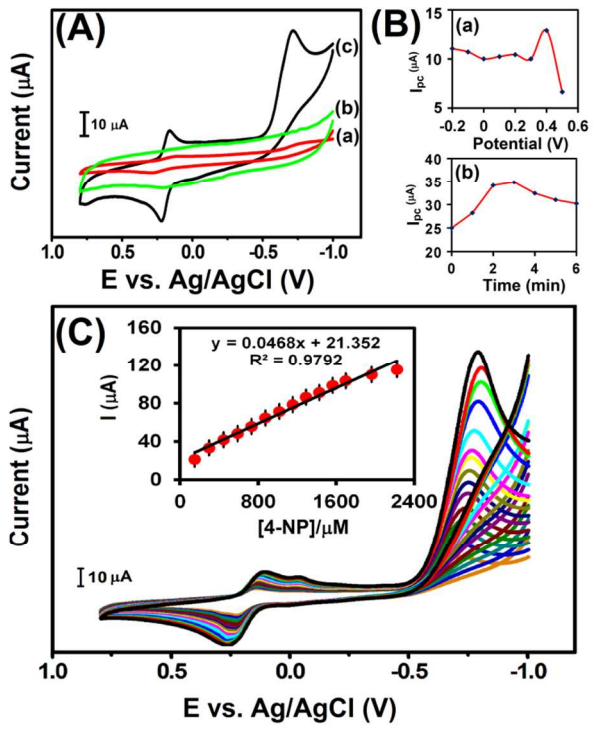

Fig. 4 (A) CV curves of (a) bare and (c) Pd/CPM-1 modified GCE in the presence of 0.3 mM 4-NP in 0.05 M acetate buffer solution (pH 5.0). Curve (b) represents profile recorded in the absence of 4-NP in the electrolyte. (B) Variations of peak current with (a) accumulated potential, and (b) time during detection of 4-NP (0.3 mM). (C) CV curves of Pd/CPM-1 modified GCE under varied 4-NP concentrations (150–2222 μM). Inset: Plot of cathodic reduction perak current (I_{pc}) *vs* 4-NP concentration.

The effect of scan rate of electrocatalytic activity of Pd/CPM-1 modified GCE for detection of 4-NP have been examined, as shown in **Fig. S5 (ESI†)**. A linear correlation between reducdtion peak current (I_{pc}) and square root of scan rate ($\upsilon^{1/2}$) is evident **(Inset, Fig. S5; ESI†)** over the range of 10–100 mV s^{-1}. This indicates the kinetics of the overall process was controlled by a diffusion process.[27] Moreover, effects of accumulation potential and time, which may affect the amount of absorbed 4-NP on the surface of the electrode, hence, the detection sensitivity and limit, were also investigated over the Pd/CPM-1 modified GCE by means of DPV method. As shown in **Fig. 4B(a)**, an optimal peak current was observed at an accumulating potential of *ca.* 0.4 V, revealing the optimal peak potential for the primary reduction peak. Likewise, an optimal peak current was observed at an retention time of ca. 3 min **(Fig. 4B(b))**, which may be ascribed due to the threshold of saturated 4-NP adsorption over the catalyst film.

To further assess the analytical performances of the proposed 4-NP sensor, electrocatalytic activities of the Pd/CPM-modified GCEs were evaluated by using CV and DPV measurements. Moreover, to avoid interference arising from foreign species (*e.g.,* ascorbic acid) during analysis of real samples,[28] catalytic test reactions were conducted at a reduction peak of –0.7 V. By adopting the above optimized parameters, CV measurements were performed over the Pd/CPM-1 modified GCE in the presence of 0.05 M acetate buffer solution with pH 5.0 under varied 4-NP concentrations (150 μM–2.2 mM), as shown in **Fig. 4C.** As expected, a much higher reduction peak current than oxidation peak current was observed. Moreover, a linear dependence of the cathodic peak current (I_{pc}) with 4-NP concentration was observed **(Inset, Fig. 4C)**. Likewise, the corresponding DPV profiles under varied 4-NP concentrations (0.3 μM –1.5 mM) are shown in **Fig. 5**. Again, a linear dependence of I_{pc} with 4-NP concentration was also observed **(Inset, Fig. 5)**. Accordingly, a detection limit and sensitivity of 0.07 μM and 0.506 μA μM^{-1} cm^{-2}, respectively, may be inferred for the Pd/CPM-modified GCE based 4-NP sensor. As summarized in **Table 3**, the Pd/CPM-modified GCE reported herein exhibits good sensitivity, and lower detection limit over a wide range of 4-NP concentration compared to various modified electrodes available in the literature.[14b,25b,29,30]

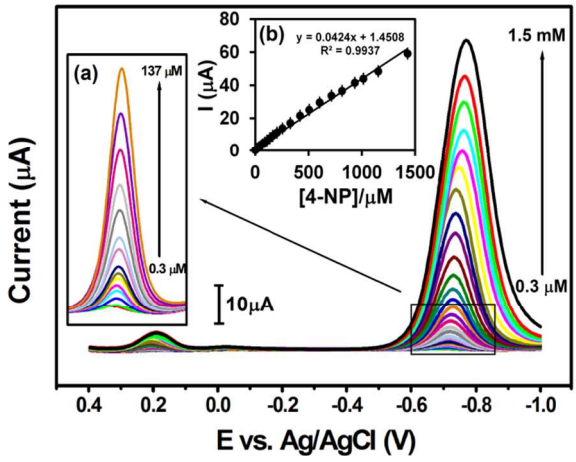

Table 3 Comparison of analytical parameters for detection of 4-NP over various modified electrodes

Modified electrode	Detection limit (μM)	Concentration range (μM)	Sensitivity ($\mu A\ \mu M^{-1}\ cm^{-2}$)	Reference
AC[a]	0.16	1–500	5.810	14b
MWCNT[b]/PDPA[c]/GCE[d]	---	8.9–1500	0.632	25b
G[e]/Nf[f]/SPCE[g]	0.6	10–620	---	29a
AuNPs[h]/GCE	8.0	10–1000	---	29b
AgNPs[i]/GCE	0.5	1.5–140	0.043	29c
AuNPs/RGO[j]	0.01	0.05–2	---	30a
HA-NP[k]/GCE	0.6	1–300	---	30b
PMB[l]/GCE	0.00009	0.015–0.250	5.9	30c
Pd/CPM-1/GCE	0.07	0.3–1500	0.506	This work

[a] AC: activated carbon. [b] MWCNT: multi-walled carbon nanotubes. [c] PDPA: poly-diphenylamine. [d] GCE: glassy carbon electrode. [e] G: graphene. [f] Nf: nafion. [g] SPCE: screen printed carbon electrode. [h] AuNPs: gold nanoparticles. [i] AgNPs: silver nanoparticles. [j] RGO: reduced graphene oxide. [k] HA-NP: hydroxyl apatite nano powder. [l] PMB: poly(methylene blue).

Fig. 5 DPV curves of Pd/CPM-1 modified GCE under varied 4-NP concentrations (0.3–1428 μM) in 0.05 M acetate buffer solution (pH 5.0). Inset: Plot of cathodic reduction perak current (I_{pc}) *vs* 4-NP concentration.

The storage stability of the reported 4-NP sensor was evaluated by performing additional CV measurements for the Pd/CPM-1 modified GCE in the presence of 0.3 mM 4-NP in N_2 saturated 0.05 M acetate buffer (pH = 5.0) while monitoring variation of the reduction peak current periodically. The sensor was found to retain *ca.* 89.4% of its initial reduction peak current after keeping the modified GCE in air at room temperature for 2 weeks (not shown), indicating an excellent storage stability. Additional CV measurements were also carried out for five different Pd/CPM-modified GCEs prepared under the same conditions. These substrates showed acceptable reproducibility with a relative standard deviation (RSD) of 2.7%. Moreover, a RSD value of 2.5% was obtained after 10 successive measurements under 0.3 mM 4-NP, indicating a good or the repeatability of the proposed sensor. Moreover, to investigate the versatile application of the 4-NP sensor for practical analysis of real samples, tap and lake water samples were analysed and the results are shown in **Table S3 (ESI†)**. It is found that satisfactory recovery rate exceeding *ca.* 98% may be inferred for these real samples, indicating promising perspective application of the preoposed 4-NP sensor for analysis of real samples.

3. Conclusions

In summary, a series of stable Pd/CPM nanocomposites with differing Pd contents for practical catalytic applications have been synthesized and thoroughly characterized by a variety of different analytical and spectroscopic techniques. The Pd/CPM ctalysts show excellent catalytic activities for reduction of 4-NP with rate constant ($k = 6.87 \times 10^{-2}\ s^{-1}$) surpassing other supported PdNP catalysts. The synthesized Pd/CPM catalysts also exhibit superior catalytic activities for C–C coupling reactions with desirable product yields > 88%. In addition, a novel 4-NP electrochemical sensor with significant electrocatalytic performance has also been developed based on Pd/CPM-modified GCE for the first time. The novel 4-NP sensor reported herein exhibits much lower detection limit, excellent durability, and high sensitivity over wide range of 4-NP concentration, surpassing other modified electrodes reported in literature. The proposed electrodes also show remarkable performances during analyses of real samples, rendering facile large-scale production and perspective practical industrial applications.

Acknowledgements

The authors are grateful to the financial supports from Academia Sinica and Ministry of Science and Technology (Contract No.: 101-2113-M-001-020-MY3), Taiwan.

References

1 (*a*) W. Li and D. Zhao, *Chem. Commun.,* 2013, **49**, 943–946. (*b*) Y. Deng, J. Wei, Z. Sun and D. Zhao, *Chem. Soc. Rev.,* 2013, **42**, 4054–4070. (*c*) G. Xie, K. Zhang, B. Guo, Q. Liu, L. Fang, and J. R. Gong, *Adv. Mater.,* 2013, **25**, 3820–3839. (d) G. Xie, K. Zhang, H. Fang, B. Guo, R. Wang, H. Yan, L. Fang, and J. R. Gong, *Chem. Asian J.,* 2013, **8**, 2395–2400.

2 (*a*) S. Tanaka, Y. Katayama, M. P. Tate, H. W. Hillhouse and Y. Miyake. *J. Mater. Chem.,* 2007, **17**, 3639–3580. (*b*) A. Y. Lo, C. T. Hung, N. Yu, C. T. Kuo and S. B. Liu, *Appl. Energy,* 2012, **100**, 66–74.

3 (*a*) S. H. Liu, W. Y. Yu, C. H. Chen, A. Y. Lo, B. J. Hwang, S. H. Chien and S. B. Liu, *Chem. Mater.,* 2008, **20**, 1622–1628. (*b*) S. H. Liu, C. C. Chiang, M. T. Wu and S. B. Liu, *Int. J. Hydrogen Energy,* 2010, **35**, 8149–8154. (*c*) Y. Fang, Y. Lv, R. Che, H. Wu, X. Zhang, D. Gu, G. Zheng and D. Zhao, *J. Am. Chem. Soc.,* 2013, **135**, 1524–1530.

4 (*a*) Y. Wan, H. Wang, Q. Zhao, M. Klingstedt, O. Terasaki and D. Zhao, *J. Am. Chem. Soc.,* 2009, **131**, 4541–4550. (*b*) Y. Lv, F. Zhang, Y. Dou, Y. Zhai, J. Wang, H. Liu, Y. Xia, B. Tu and D. Zhao, *J. Mater. Chem.,* 2012, **22**, 93–99.

5 (*a*) Z. Sun, B. Sun, M. Qiao, J. Wei, Q. Yue, C. Wang, Y. Deng, S. Kaliaguine and D. Zhao, *J. Am. Chem. Soc.,* 2012, **134**, 17653–17660. (*b*) Z. Wang, C. Xu, G. Gao and X. Li, *RSC Adv.,* 2014, **4**, 13644–13651. (*c*) X. Gu, W. Qi, X. Xu, Z. Sun, L. Zhang, W. Liu, X. Pan and D. Su, *Nanoscale,* 2014, **6**, 6609–6616. (*d*) Y. Chi, J. Tu, M. Wang, X. Li, and Z. Zhao, *J. Colloid Inter. Sci.,* 2014, **423**, 54–59.

6 (*a*) P. Gao, A. Wang, X. Wang and T. Zhang, *Catal. Lett.,* 2008, **125**, 289–295. (*b*) J. Kang, O. L. Li and N. Saito, *Nanoscale,* 2013, **5**, 6874–6882.(*c*) Y. Yang, Y. Ren, C. Sun and S. Hao, *Green Chem.,* 2014, **16**, 2273–2280.

7 (*a*) P. Gao, A. Wang, X. Wang, and T. Zhang, *Chem. Mater.,* 2008, **20**, 1881–1888. (*b*) J. Li, J. Gu, H. Li, Y. Liang, Y. Hao, X. Sun and L. Wang, *Micropor. Mesopor. Mater.,* 2010, **128**, 144–149. (*c*) W. Wang, H. Y. Wang, W. Wei, Z. G. Xiao and Y. Wan, *Chem. Eur. J.,* 2011, **17**, 13461–13472. (*d*) J. Choma, K. Jedynak, M. Marszewski and M. Jaroniec, *Appl. Surf. Sci.,* 2012, **258**, 3763–3770. (*e*) A. Garcıa, A. Nieto, M. Vila and M. Vallet-Regi, *Carbon,* 2013, **15**, 410–418.

8 (*a*) D. Saha and S. Deng, *Langmuir,* 2009, **25**, 12550–12560. (*b*) X. Xu, Y. Li, Y. Gong, P. Zhang, H. Li and Y. Wang, *J. Am. Chem. Soc.,* 2012, **134**, 16987–16990.

9 (*a*) X. Sun and Y. Li, *Angew. Chem. Int. Ed.,* 2004, **43**, 597–601. (*b*) H. Lee, S. M. Dellatore, W. M. Miller and P. B. Messersmith, *Science,* 2007, **318**, 426–430. (*c*) S. Ikeda, K. Tachi, Y. H. Ng, Y. Ikoma, T. Sakata, H. Mori, T. Harada and M. Matsumura, *Chem. Mater.,* 2007, **19**, 4335–4340. (*d*) R. J. White, K. Tauer, M. Antonietti and M. M. Titirici, *J. Am. Chem. Soc.,* 2010, **132**, 17360–17363. (*e*) B. Hu, K. Wang, L. Wu, S. H. Yu, M. Antonietti and M. M. Titirici, *Adv. Mater.,* 2010, **22**, 813–828.

10 (*a*) S. H. Liu, R. F. Lu, S. J. Huang, A. Y. Lo, S. H. Chien and S. B. Liu, *Chem. Commun.,* 2006, 3435–3437. (*b*) A. Postma, Y. Yan, Y. J. Wang, A. N. Zelikin, E. Tjipto and F. Caruso, *Chem. Mater.,* 2009, **21**, 3042–3044. (*c*) L. Liu, F. Y Wang, G. S. Shao, T. Y. Ma and Z. Y. Yuan, *Carbon,* 2010, **48**, 2644–2673. (*d*) H. Jiang, L. Yang, C. Li, C. Yan, P. S. Lee and J. Ma, *Energy Environ. Sci.,* 2011, **4**, 1813–1819. (*e*) C. M. Ghimbeu, L. Vidal, L. Delmotte, J. M. L. Meins and C. Vix-Guterl, *Green Chem.,* 2014, **16**, 3079–3088.

11 (*a*) R. J. Kalbasi and N. Mosaddegh, *Mater. Chem. Phys.,* 2011, **130**, 1287–1293. (*b*) H. R. Choi, H. Woo, S. Jang, J. Y. Cheon, C. Kim, J. Park, K. H. Park and S. H. Joo, *ChemCatChem.,* 2012, **4**, 1587–1594. (*c*) P. Veerakumar, M. Velayudham, K. L. Lu and S. Rajagopal, *Appl. Catal., A,* 2013, **455**, 247–260.

12 (*a*) Z. Li, J. Liu, C. Xia and F. Li, *ACS Catal.,* 2013, **3**, 2440–2448. (*b*) P. Zhang, Y. Gong, H. Li, Z. Chen and Y. Wang, *Nat. Commun.,* 2013, **4**, 1593–1603. (*c*) L. Ma, D. Chu and R. Chen, *Int. J. Hydrogen Energy*, 2012, **37**, 11185–11194. (*d*) X. Ji, K. T. Lee, R. Holden, L. Zhang, J. Zhang, G. A. Botton, M. Couillard and L. F. Nazar, *Nat. Chem.,* 2010, **2**, 286–293.

13 (*a*) C. Liang and S. Dai, *J. Am. Chem. Soc.,* 2006, **128**, 5316–5317. (*b*) X. Wang, J. S. Lee, C. Tsouris, D. W. DePaoli and S. Dai, *J. Mater. Chem.,* 2010, **20**, 4602–4608. *(c*) R. Liu, S. M. Mahurin, C. Li, R. R. Unocic, J. C. Idrobo, H. Gao, S. J. Pennycook and S. Dai, *Angew. Chem. Int. Ed.,* 2011, **50**, 6799–6802.

14 (*a*) B. Devadas, M. Rajkumar, S. M. Chen and P. C. Yeh, *Anal. Methods,* 2014, **6**, 4686–4691. (*b*) R. Madhu, C. Karuppiah, S. M. Chen, P. Veerakumar and S. B. Liu, *Anal. Methods*, 2014, **6**, 5274–5280. (*c*) P. Veerakumar, R. Madhu, S. M. Chen, C. T. Hung, P. H. Tang, C. B. Wang and S. B. Liu, *Analyst*, 2014, in press (DOI**:** 10.1039/C4AN01083C).

15 (*a*) T. Vincent and E. Guibal, *Langmuir,* 2003, **19**, 8475–8483. (*b*) S. Panigrahi, S. Basu, S. Praharaj, S. Pande, S. Jana, A. Pal, S. K. Ghosh and T. Pal, *J. Phys. Chem. C*, 2007, **111**, 4596–4605. (*c*) M. J. Vaidya, S. M. Kulkarni, R. V. Chaudhari, C. V. Rode, M. J. Vaidya, R. V. Chaudhari, *Org. Process Res. Dev.,* 1999, **3**, 465–470. (*d*) N. Comisso, S. Cattarin, S. Fiameni, R. Gerbasi, L. Mattarozzi, M. Musiani, L.Vázquez-Gómez and E. Verlato, *Electrochem. Commun.,* 2012, **25**, 91–93.

16 (*a*) K. B. Narayanan and N. Sakthivel, *J. Hazard. Mater.* 2011, **189**,

519–525. (*b*) T. L. Lai, K. F. Yong, J. W. Yu, J. H. Chen, Y. Y. Shu and C. B. Wang, *J. Hazard. Mater.,* 2011, **185**, 366–372. (*c*) D. Makovec, M. Sajko, A. Selišnik and M. Drofenik, *Mater. Chem. Phys.,* 2011, **129**, 83–89.

17 (*a*) Y. Meng, D. Gu, F. Zhang, Y. Shi, L. Cheng, D. Feng, Z. Wu, Z. Chen, Y. Wan, A. Stein and D. Zhao, *Chem. Mater.,* 2006, **18**, 4447–4464. (*b*) P. Dauthal and M. Mukhopadhyay, *Ind. Eng. Chem. Res.,* 2013, **52**, 18131–18139.

18 M. Ignat, C. J. Van Oers, J. Vernimmen, M. Mertens, S. Potgieter-Vermaak, V. Meynen, E. Popovici and P. Cool, *Carbon*, 2010, **48**, 1609–1618.

19 (*a*) P. Veerakumar, M. Velayudham, K. L. Lu and S. Rajagopal, *Appl., Catal., A,* 2013, **439–440**, 197–205. (*b*) J. Feng, L, Su, Y. Ma, C. Ren, Q. Guo and X. Chen, *Chem. Eng. J.,* 2013, **221**, 16–24. (*c*) K. Mondal, J. Kumar, A. Sharma, *Colloids and Surf., A,* 2013, **427**, 83–94.

20 (*a*) X. Wu, C. Lu, W. Zhang, G. Yuan, R. Xiong and X. Zhang, *J. Mater. Chem. A,* 2013, **1**, 8645–8652. (*b*) Y. Peng, X. Wu, L. Qiu, C. Liu, S. Wang and F. Yan, *J. Mater. Chem. A*, 2013, **1**, 9257–9263.

21 (*a*) H. Li, L. Han, J. Cooper-White and I. Kim, *Green Chem.,* 2012, **14**, 586–591. (*b*) Y. Fang and E. Wang, *Nanoscale,* 2013, **5**, 1843–1848. (c) H. K. He and C. Gao, *Molecules,* 2010, **15**, 4679–4694. (*d*) Z. Zhang, F. Xiao, J. Xi, T. Sun, S. Xiao, H. Wang, S. Wang and Y. Liu, *Sci. Rep.,* 2013, **4**, 4053–4057. (*e*) W. Sun, X. Lu, Y. Tong, Z. Zhang, J. Lei, G. Nie and C. Wang, *Int. J. Hydrogen Energy,* 2014, **39**, 9080–9086. (*f*) J. Sun, Y. Fu, G. He, X. Sun and X. Wang, *Catal. Sci. Technol.,* 2014, **4**, 1742–1748.

22 (*a*) A. Corma, P. Conception and P. Serna, *Angew. Chem. Int. Ed.,* 2007, **46**, 7266–7269. (*b*) S. Jana, S. K.Ghosh, S. Nath, S. Pande, S. Praharaj, S. Panigrahi, S. Basu and T. Endo, T. Pal, *App. Catal. A* 2006, **313**, 41–48. (*c*) S. Wunder, F. Polzer, Y. Lu, Y. Mei and M. Ballauff, *J. Phys. Chem. C,* 2010, **114**, 8814–8820. (*d*) B. Baruah, G. J. Gabriel, M. J. Akbashev, and M. E. Booher, *Langmuir,* 2013, **29**, 4225–4234.

23 (*a*) M. N. Nadagouda, V. Polshettiwar and R. S. Varma, *J. Mater. Chem.,* 2009, **19**, 2026–2031. (*b*) M. Perez-Lorenzo, *J. Phys. Chem. Lett.,* 2012, **3**, 167–174.

24 L. Q. Luo, X. L. Zoua, Y. P. Ding and Q. S. Wu, *Sens. Actuators, B*, 2008, **135**, 61–65.

25 (*a*) F. C. Moraes, S. T. Tanimoto, G. R. S. Banda, S. A. S. Machado and L. H. Mascaro, *Electroanal.,* 2009, **21**, 1091–1098. (*b*) Y. L. Yang, B. Unnikrishnan and S. M. Chen, *Int. J. Electrochem. Sci.,* 2011, **6**, 3902–3912.

26 M. A. E. Mhammedi, M. Achak, M. Bakasse and A. Chtaini, *J. Hazard. Mater.,* 2009, **163**, 323–328.

27 K. C. Honeychurch and J. P. Hart, *Electroanal.,* 2007, **19**, 2176–2184.

28 G. S. Garbellini, G. R. Salazar-Banda and L. A. Avaca, *Food Chem.,* 2009, **116**, 1029–1035.

29 (*a*) A. Arvinte, M. Mahosenaho, M. Pinteala, A. M. Sesay and V. Virtanen, *Microchim. Acta.,* 2011, **174**, 337–343. (*b*) L. Chu, L. Han and X. Zhang, *J. Appl. Electrochem.,* 2011, **41**, 687–694. (*c*) I. G. Casella and M. Contursi, *J. Electrochem.Soc.,* 2007, **154**, 697–702.

30 (*a*) Y. Tang, R. Huang, C. Liu, S. Yang, Z. Lu and S. Luo, *Anal. methods,* 2013, **5**, 5508–5514. (*b*) H. Yin, Y. Zhou, S. Ai, X. Liu, L. Zhu and L. Lu, *Microchim. Acta.,* 2010, **169**, 87–92. (*c*) K. Giribabu, R. Suresh, R. Manigandan, S. Munusamy, S. Praveen Kumar, S. Muthamizh and V. Narayanan, *Analyst,* 2013, **138**, 5811–5818.

Graphical Abstract

Title: Highly stable and active palladium nanoparticles supported on porous carbons for practical catalytic applications

Authors: Pitchaimani Veerakumar, Rajesh Madhu, Shen-Ming Chen, Vediyappan Veeramani, Chin-Te Hung, Pi-Hsi Tang, Chen-Bin Wang and Shang-Bin Liu

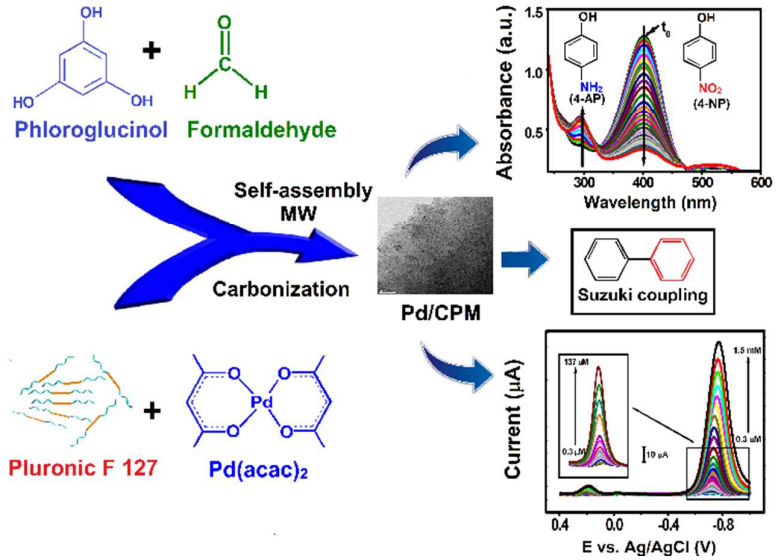

Carbon porous materials containing highly dispersed Pd nanoparticles show superior performances during catalytic reduction of 4-nitrophenol (4-NP), C-C coupling reaction, and electrochemical detection of 4-NP.